ARTICLES

Ab Initio Study of Temperature and Pressure Dependence of Energy and Phonon-Induced Dephasing of Electronic Excitations in CdSe and PbSe Quantum Dots†

Hideyuki Kamisaka,*,‡,§ Svetlana V. Kilina,‡,|| Koichi Yamashita,§ and Oleg V. Prezhdo‡

Department of Chemistry, University of Washington, Seattle, Washington 98195, Department of Chemical System Engineering, The University of Tokyo, 7-3-1 Hongo, Bunkyo-ku, Tokyo 113-8656, Japan, and Theory Division, Los Alamos National Lab, Los Alamos, New Mexico 87545

Received: October 29, 2007; Revised Manuscript Received: January 12, 2008

The pressure and temperature dependence of the lowest excitation energy of PbSe ($Pb_{68}Se_{68}$, $d = 2.0$ nm) and CdSe ($Cd_{33}Se_{33}$, $d = 1.6$ nm) quantum dots (QDs) were investigated by *ab initio* density functional theory and molecular dynamics simulation. Additionally, pure-dephasing/decoherence induced by the electron–phonon interaction was studied using optical response theory for several pairs of electronic states, including ground, excitonic and biexcitonic states. Linear dependence on temperature was observed for all quantities under consideration. The results were consistent with other theoretical and experimental reports. The *ab initio* data was analyzed using the effective mass approximation and the hyperbolic band model. The analysis confirmed the temperature dependence of the effective mass in the PbSe QD, as suggested in a recent experimental report [Liptay, T. J.; Ram, R. J. *Appl. Phys. Lett.* **2006**, *89*, 223132].

Introduction

Nanometer-size structures whose spatial extent is limited to few dimensions, a layer (2D), a wire (1D), or a dot (0D), exhibit unique electronic, mechanical, and chemical properties. Quantum confinement of electrons in semiconductor quantum dots (QDs) in particular gives rise to novel phenomena, such as phonon-bottleneck,[1] and Coulomb[2] and spin[3] blockades. QDs can be exploited in many electronic devices including lasers,[4] light emitting diodes,[5] and field effect transistors.[6] In addition to the new physics, QDs provide the unique opportunity for control of their properties with a simple change of shape and size. Recent advances in synthetic procedures make it possible to limit the QD size distribution to within 7%.[7] QDs are sometimes regarded as artificial atoms and are considered to be the basic building blocks of electronic and optical devices of the future.

CdSe QDs are among the most intensely investigated semiconductor QDs. The relatively small band gap of CdSe allows realization of various optical devices within the visible light range. For this reason, the optical properties of CdSe QDs, including excited-state lifetimes[8] and absorption[9] and luminescence[10] spectra, have been surveyed in a large number of papers. QDs made of PbSe are very interesting due to the extremely strong quantum confinement effects and a rare symmetry between the electron and hole band structures.[11] These features of PbSe QDs have created distinct conditions for the generation of multiple excitons (MEs) upon absorption of just a single photon.[12–17] MEs provide an opportunity for a large increase in the efficiency of QD-based photovoltaic devices relative to the conventional materials that utilize only one exciton per absorbed photon.

The pressure and temperature dependence of the QDs made of CdSe, PbSe, and related materials have received much recent attention. The QD optical spectra under hydrostatic pressure was reported for CdSe,[18,19] core/shell CdSe/ZnS,[20] and PbSe.[21] The lowest excitation energy (E_g) was measured for CdSe,[22–24] CdSe/ZnS,[25] PbSe,[26] PbS,[26,27] CdS[28] QDs over wide temperature ranges, and linear temperature dependence of the first absorption peak was reported. Particularly interesting is the observation of the opposite sign in the variation of the lowest excitation energy with temperature (dE_g/dT) in small PbS QDs relative to bulk PbS.[27] The dE_g/dT values show strong dependence on the PbS QD size, changing sign from negative for $d \leq 4$ nm to positive for $d \geq 4$ nm.[26]

The temperature dependence of the band gap of bulk semiconductors was thoroughly investigated in the condensed matter physics community in the 1960–70s. Following the introduction of the well-known Fröhlich Hamiltonian, Fan[29] pioneered a perturbative treatment of the electron–phonon coupling in the standard band model and derived an expression for dE_g/T through a self-energy term of electrons. The theory successfully explained the temperature dependence of the gap in bulk silicon and germanium. However, the theory was limited to negative values of dE_g/dT and was not applicable to systems such as bulk PbTe which showed positive dE_g/dT. The first theoretical explanation of the positive dE_g/dT was given by Keffer and co-workers.[30] Their pseudopotential formalism included the electron–phonon interaction not only to the first, but also to the second order, which was related to the Debye–Waller factor. The theory both explained the temperature dependence of the PbTe gap[31] and was applicable to silicon and germanium.[32]

† Part of the "Larry Dalton Festschrift".

* To whom correspondence should be addressed. E-mail: kami@tcl.t.u-tokyo.ac.jp.

‡ University of Washington.

§ The University of Tokyo.

|| Los Alamos National Lab.

10.1021/jp710435q CCC: $40.75
Published on Web 05/07/2008

Compared to these mature theoretical treatments of bulk systems, the theory for the temperature dependence of the first absorption peak energy is much less established with QDs. Recently, Olkhovets et al.[26] proposed a simple expression, in which the temperature dependence of the lowest excitation energy arises from a combination of the following four factors: (i) dilation of the lattice, (ii) thermal expansion of the envelope function, (iii) change in the Coulomb interaction, and (iv) change in the electron–phonon coupling. The analysis implicitly assumes additivity and separability of these four effects. According to this report, the most dominant contribution to the temperature dependence of the electronic excitation energy is due to the electron–phonon coupling. Later, Liptay et al.[33] advocated an improved version of the expression, incorporating the temperature dependence of the exciton effective mass.

The electron–phonon interaction is responsible for a number of other important processes that occur in QDs, including electronic energy loss and decoherence. Loss of coherence between superpositions of electronic energy levels has important implications for quantum computing.[34] Electronic and spin states of QDs can be used to encode qubits, with the current realization mainly limited to nuclear spins. Phonon-mediated spin relaxation and its decoherence due to the spin–orbit coupling (SOC) is studied both experimentally[35] and theoretically.[36,37] Interaction with nuclear spins induces decoherence of electronic spins.[37] At low temperatures, decoherence of electronic states occurs through virtual phonons, leading to a long coherence time which is essential for quantum computation. Decoherence manifests itself spectroscopically as the pure-dephasing contribution to the optical absorption linewidths.[38] Processes mediated by virtual phonons determine the width of the sharp peak seen at low temperatures on top of a broad pedestal.[39] The peak is known as zero phonon line (ZPL). The pedestal part of the absorption line is generated by thermal phonon processes. Several theoretical works analyze ZPL,[40] including the size and temperature dependence of ZPL in CdSe QDs.[41]

Phonon-induced electronic dephasing is an important factor in the generation of MEs, which can substantially raise the efficiency of QD solar cells.[12–17] The microscopic mechanism of this process remains an open question and is highly debated from different perspectives.[12–15,17] One of the proposed mechanisms explains the appearance of MEs by their faster dephasing relative to single excitons.[13] Another mechanism based on the inverse Auger effect assumes an incoherent rate process with rapid dephasing.[12] The direct mechanism postulates that MEs are formed nearly instantaneously and faster than decoherence.[16] Unlike the ZPL phenomenon which occurs at low temperatures, the dominant contribution to the decoherence process that is relevant for MEs comes from the vibrationally induced fluctuation of the energy difference between the electronic states at room temperature.

Recently, we investigated the coherence loss involving several types of electronic states - ground, excitonic, and biexcitonic, using *ab initio* molecular dynamics (MD) data within the framework of the optical response function and semiclassical formalisms.[42] The study was limited to PbSe QDs at room temperature. Currently, we extend our earlier study to CdSe QDs and a wide temperature range. The results are compared with other reports and theoretical models, and the qualitative difference between the two QD materials is discussed in detail. In addition to decoherence, we thoroughly investigate the temperature and pressure dependence of the band gaps in both QDs and the related bulk materials.

The paper is arranged as follows. The next section explains the technical details of the *ab initio* MD calculations and briefly reviews the method for estimating the decoherence time. The data are presented and compared with the existing reports in the Results section, starting with the temperature and pressure dependence of the band gap and continuing with the analysis of the quantum coherence loss. The Discussion relates the results of the atomistic simulations to the two analytical models for the quantum confinement energy. The paper concludes with a summary of the key observations.

Simulation Details

The bulk structures of the CdSe and PbSe were prepared first. Bulk CdSe and PbSe has the wurtzite structure ($a = 4.30$ Å and $c = 7.01$ Å)[43] and the rocksalt structure ($a = 6.1169$ Å),[44] respectively. Two stoichiometric spherical QDs were cut from bulk: $Cd_{33}Se_{33}$ ($d = 1.6$ nm) and $Pb_{68}Se_{68}$ ($d = 2.0$ nm). The latter dot is identical to one of the dots which we used in our previous paper.[42]

The electronic structure calculations, structural optimizations and molecular dynamics were performed using density functional theory (DFT)[45] in the Kohn–Sham (KS) representation.[46] The PW91 density functional[47] was used throughout of the study. The core–electrons were represented with the Vanderbilt ultrasoft pseudopotentials (USPP),[48] as described in ref 49 The KS orbitals were expanded using the plane wave basis set with the energy cutoff of 12.34 (8.55) Ry for CdSe (PbSe) QD. Since these QDs are not extended systems, the only **k**-point sampled was the Γ point. The calculations were performed with Vienna *Ab initio* Simulation Package (VASP).[50]

The geometries of the QDs were optimized at $T = 0$ K. In order to study the effect of hydrostatic pressure on the QD properties, the electronic structure calculations were carried out for stretched and compressed dots with dilations of +1.0%, +0.5%, –0.5%, and –1.0%. The dilated structures were generated from the optimized structure. The bulk modulus of the CdSe bulk is anisotropic. The ratio of the compression coefficients between the two axes is $a/c = 1.6$.[43] Since the CdSe QD cannot be ideally symmetric as seen in Figure 1, we used isotropic dilation. The band gap of the dots was approximated by the difference in the energies of the lowest unoccupied molecular orbital (LUMO) and the highest occupied molecular orbital (HOMO).

The effect of the lattice dilation was also investigated in bulk by imposing an isotropic external stress of +5.0, +2.5, –2.5, and –5.0 GPa. The CdSe wurtzite structure was used at all pressures; however, it should be noted that bulk CdSe converts to the rocksalt structure at a pressure near 3 GPa.[51] In the bulk calculations, the cutoff energy was raised to 11.41 Ry for PbSe, and the **k** points were sampled according to Γ-centered Monkhorst-Pack[52] $8 \times 8 \times 8$ scheme for both materials. The band gap was taken at the Γ- and L-points for CdSe[53] and PbSe,[54] respectively. These two **k** points are known to give the band gap in these semiconductors.

It has been established that SOC is important in the calculation of the absolute value of the band gap of bulk PbSe.[55] In contrast, the electronic structure of PbSe QDs is dominated by quantum confinement. The exciton localization length in bulk PbSe is 46 nm.[11] This is more than an order of magnitude larger than a typical QD size. Since the present study focuses on QDs rather than bulk PbSe, SOC was not included in the calculation. Still, even in bulk, the temperature dependence of the PbSe band gap is not significantly influenced by SOC. The situation was clearly exemplified for PbS, which has a similar band structure

to PbSe.[21] SOC lowers the band gap of bulk PbS, bringing it closer to the experimental value. The magnitude of the gap decreases because the valence band maximum (VBM) and the conduction band minimum (CBM) split due to SOC.[21] However, the VBM and CBM do not interact with each other through SOC,[55] since they have different symmetries (L_{1v} and L'_{2c}).[54] Moreover, the bulk lattice constants can be reproduced without SOC. As a result, the dE_g/dP dependence of bulk PbSe can be obtained without SOC. The pressure dependence of the gap of bulk PbSe, dE_g/dP, is reproduced better at the GGA level, if SOC is omitted.[21] Only a minor modification of the splitting of VBM and CBM under external pressure can be seen in Figure 1d of ref 56. Therefore, it is reasonable to expect that the change of E_g can be obtained in the present calculation scheme not only for the QDs but also for the bulk materials, even though there may be a considerable error in the absolute value of the gap for bulk PbSe.

Ab initio MD simulations were performed with the two QDs at three different temperatures. First, the QDs optimized at $T = 0$ K were heated to 300 K by repeated velocity rescaling. The Hellman-Feynman forces on the nuclei were calculated, and the integration of the classical motion of the nuclei was carried out using the Verlet algorithm with the time step of 3 fs (2 fs) for the CdSe (PbSe) QD. After the equilibration, the MD simulations were continued microcanonically. The equilibration at $T = 100$ and 200 K was performed by cooling the 300 K trajectory using velocity rescaling, and the same protocol was used for the microcanonical MD simulations after the cooling.

The QD band gaps were calculated by averaging the HOMO–LUMO gap over the microcanonical trajectories. Similarly, the energy difference between the ground, excitonic, and biexcitonic states were estimated from the KS orbital energies and the occupation numbers. The same pairs of the electronic states as those in ref 42 were investigated. The unnormalized autocorrelation function of the energy difference $\Delta E(t)$ was calculated as

$$C(t) = \langle \Delta E(t)\, \Delta E(0) \rangle_{\mathrm{T}} \tag{1}$$

where the angular brackets denote microcanonical averaging. The pure-dephasing/decoherence time between the electronic state pairs was estimated using the optical response theory. The response function was computed either by direct evaluation

$$D(t) = \mathrm{e}^{i\omega t} \left\langle \exp\left(-\frac{i}{\hbar} \int_0^t \Delta E(t)\, \mathrm{d}t \right) \right\rangle_{\mathrm{T}} \tag{2}$$

or with use of the second order cumulant expansion

$$D(t) = \exp\left(-\int_0^t \mathrm{d}\tau_1 \int_0^{\tau_1} \tau_2 C(\tau_2) \right) \tag{3}$$

In the following, the units for energy, temperature, length, pressure, and frequency were eV, K, nm (=10 Å), GPa (=10 kBar), and cm^{-1}. Other units are combinations of these, with exception to the temperature dependence of the energy, which is shown in meV/GPa (=0.1 eV/Mbar) and meV/K.

Results

The structure of the CdSe QD optimized at $T = 0$ K is depicted in Figure 1. Thermal fluctuations of the atomic positions were small during the MD simulations, and the QD structures along the MD trajectories at different temperatures were quite similar. The bottom of Figure 1 shows snapshots of the HOMO and LUMO electron densities at a certain time during the simulation at $T = 300$ K. Due to the small size of the dot and the thermal atomic fluctuation, both HOMO and LUMO had complicated structure and did not show any clear symmetry as assumed in analytic models. The same situation was found for the PbSe QD.[42,57]

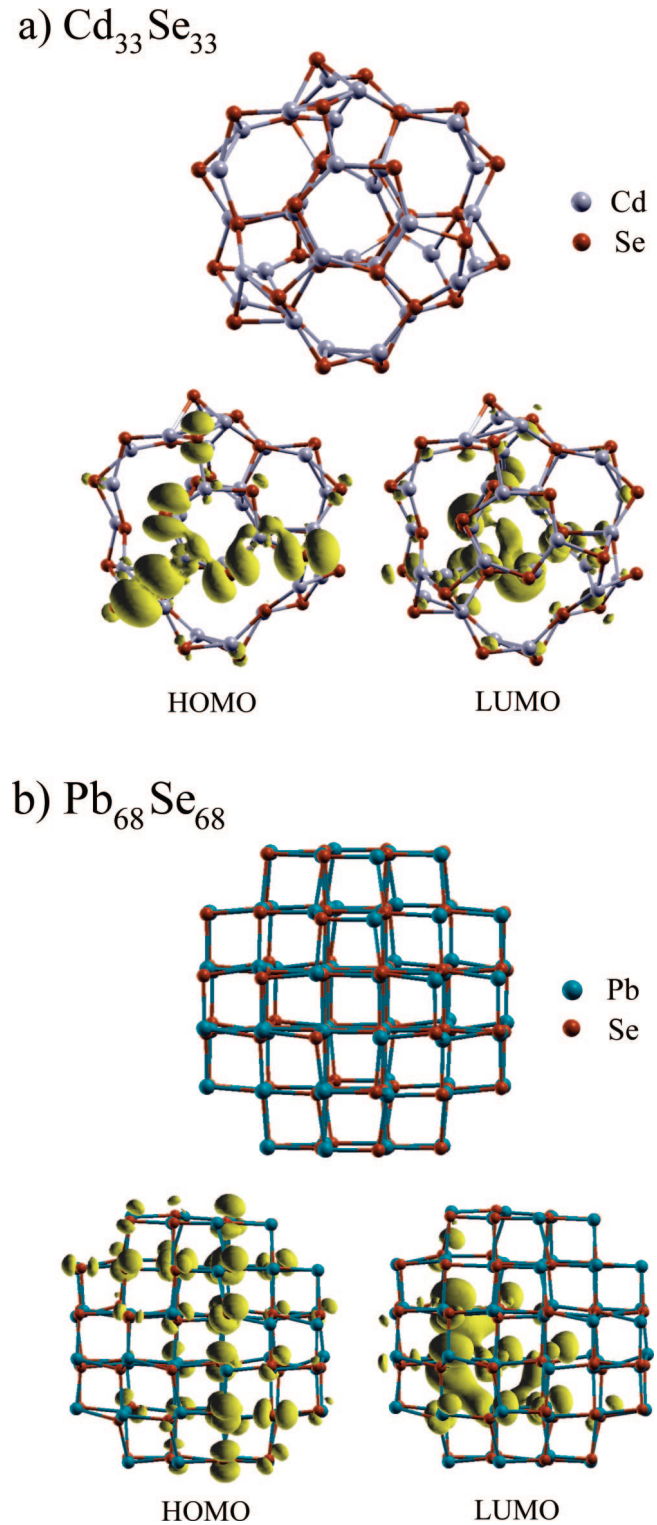

Figure 1. Structure of (a) $Cd_{33}Se_{33}$ and (b) $Pb_{68}Se_{68}$ optimized at $T = 0$ K (top) and images of HOMO and LUMO taken at a random time from a trajectory at $T = 300$ K (bottom).

Figure 2 depicts the radial distribution function (RDF) of the electron density of HOMO and LUMO measured from the center of the CdSe and PbSe QDs. Except for $T = 0$ K, these plots are made by averaging over several RDFs created at randomly chosen times along the trajectory. The shell-like structure of

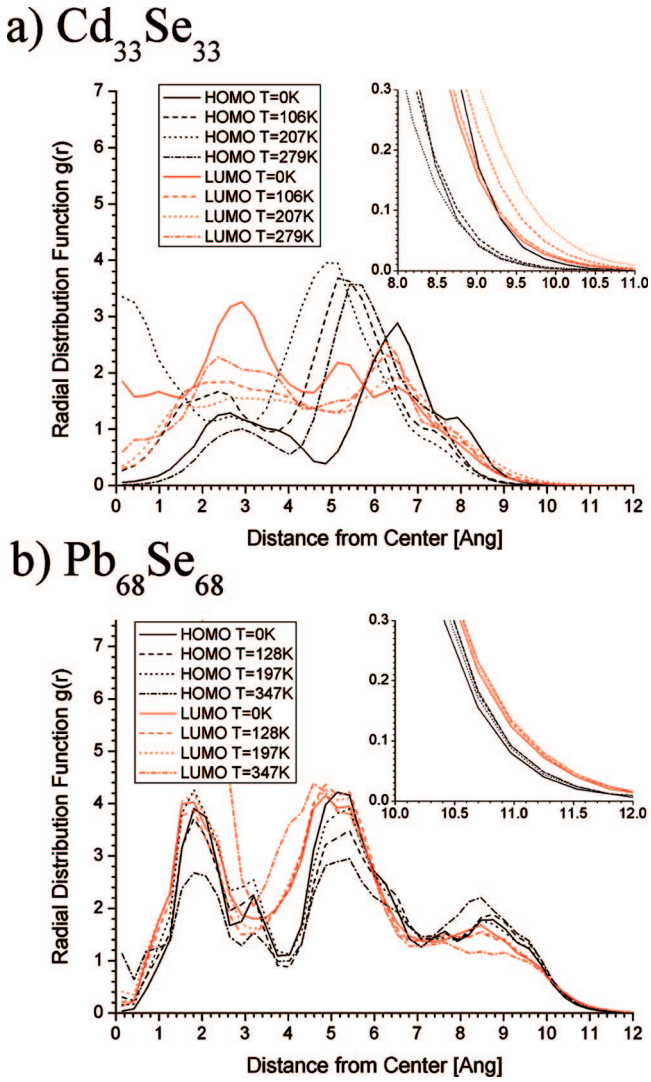

Figure 2. Radial distribution functions (RDFs) of the HOMO and LUMO electronic densities in the $Cd_{33}Se_{33}$ and $Pb_{68}Se_{68}$ QDs. The distance is measured from the dot center-of-mass. The units of RDF are such that the integral of $\rho g(r)\ \pi r^2$ gives the number of electrons, which includes both spin orientations and is equal to 2. The average electron density ρ was taken from the bulk.

the electron density in Figure 2 originates from the geometric structure of the QDs. Note that the behavior near the origin has little meaning due to the small volume element in the average and the complicated structure of the orbitals, especially for $T = 0$ K where only a single structure was used. In the CdSe QD, the LUMO tends to localize on the inner shell, whereas the HOMO localizes on the outer shell. The insets in Figure 2 show the detailed behavior of the RDFs in the long-range region. In both QDs, the LUMOs have slightly longer tails than the HOMOs. However, since the effect of the surroundings, such as a molecular surfactant or a shell of another semiconductor, was not included in the calculations, this finding should not be generalized directly. The tails of the HOMO and LUMO show complicated temperature dependence. The experimental thermal dilation coefficient for bulk CdSe is 7.4×10^{-6} K^{-1}.[58] The value for bulk PbSe is 2×10^{-5} K^{-1}.[31] According to these values, heating from 0 to 300 K dilates the dots by around 0.22% for CdSe and 0.6% for PbSe.

Figure 3 shows the band gap E_g in the bulk materials under pressure. The results are summarized in Table 1 together with the bond lengths and lattice constants. dE_g/dP is

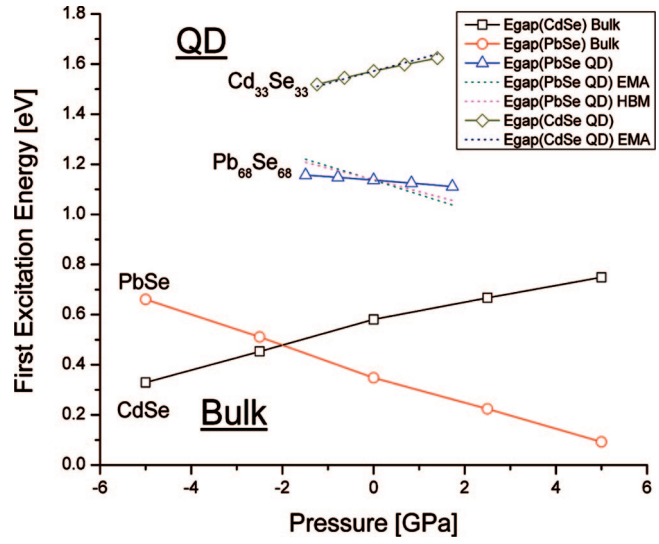

Figure 3. First excitation energies of the CdSe and PbSe QDs and corresponding bulk materials as functions of pressure. The symbols connected with the solid lines represent the results of the first-principle calculations. The dotted lines are the estimates obtained with the EMA and HBM models.

42.0 meV/GPa for bulk CdSe and –56.9 meV/GPa for bulk PbSe. The experimental measurements for bulk CdSe reported values of 33[51] and 43.1 meV/GPa,[59] and a theoretical calculation reported a value of 39 meV/GPa.[21] Our results are in good accordance with these values. On the contrary, our calculation of dE_g/dP for bulk PbSe underestimated the experimental value of –76.9,[60] –86,[61] and –91.0 meV/GPa.[62] However, other theoretical calculations also reported smaller dE_g/dP for this system: –51.8,[54] –56,[21] and –73.1[56] meV/GPa. Our value of –56.9 meV/GPa is consistent with these theoretical reports.

The band gaps calculated for the QDs with several lattice dilations are summarized in Table 2. The pressures corresponding to the dilations are also listed in the table. These pressures were estimated using the Birch–Murnaghan equation of state with the parameters taken from bulk: $B = 53.6$ (43.9) GPa and $B' = 4.57$ (3.73) for CdSe (PbSe) from refs 21 and 63. The QD results are summarized in Figure 3 together with the bulk data. Our calculations predict dE_g/dP in the CdSe and PbSe QDs are 39.8 and –14.3 meV/GPa, respectively. The signs of these values are the same as in the bulk, but in the case of the PbSe QD, the absolute magnitude is smaller than that for the bulk. The experimental value of –47 meV/GPa was reported in ref 21 for the PbSe QD with diameter $d = 3$ nm for pressures in the range of $P = 0$–5 GPa. This magnitude of dE_g/dP is smaller for the 3 nm QD than for bulk. Our magnitude calculated for the 2 nm QD is even smaller and is consistent with the experimental trend. Unlike PbSe, the literature data on dE_g/dP vary substantially for CdSe QDs. While an earlier paper reported 27 meV/GPa[18] ($d = 4.8$ nm, $P = 0$–5.2 GPa), which is smaller than the bulk value, the later experiments reported 82 meV/GPa[19] ($d = 4.5$ nm, $P = 0$–0.3 GPa), which is larger than the bulk value. A value of 45 meV/GPa, which is close to the bulk, was reported for CdSe/ZnS QD ($d = 4.4$ nm, $P = 0$–16 GPa) in the most recent paper.[20]

The temperature dependence of the band gap in the QDs is illustrated in Figure 4. The temperatures are computed based on the average kinetic energy of the atoms during the simulation. The values differ from the prescribed 100, 200, and 300 K due to finite system size. They are listed in Table 3 together with the band gaps. Linear dependence of the band gaps on temperature

TABLE 1: Calculated Lattice Constants and Band Gaps of Bulk CdSe and PbSe under External Pressure[a]

	CdSe					PbSe	
P [GPa]	r_1(Cd−Se)	r_2(Cd−Se)	a	c	E_g [eV]	r(Pb−Se)	E_g [eV]
−5.0	2.7716	2.7776	4.5281	7.3962	0.329	3.2185	0.661
−2.5	2.7200	2.7253	4.4434	7.2582	0.453	3.1478	0.511
0.0	2.6695	2.6746	4.3609	7.1234	0.581	3.0882	0.348
2.5	2.6361	2.6413	4.3064	7.0344	0.667	3.0494	0.224
5.0	2.6051	2.6100	4.2556	6.9516	0.749	3.0125	0.092

[a] All lengths are in Å. Bulk CdSe has equal number of r_1 and r_2 bonds. The lattice constant of PbSe is twice the r(Pb−Se) distance.

TABLE 2: Simulated Pressure Dependence of the Band Gap of the CdSe and PbSe QDs[a]

	CdSe QD			PbSe QD		
dilation	P [GPa]	⟨r(Cd−Se)⟩ [Å]	E_g [eV]	P [GPa]	⟨r(Pb−Se)⟩ [Å]	E_g [eV]
−1.0%	1.40	2.7162	1.624	1.73	3.0232	1.111
−0.5%	0.68	2.7299	1.598	0.83	3.0385	1.125
0%	0.0	2.7437	1.572	0.0	3.0578	1.137
+0.5%	−0.64	2.7574	1.545	−0.78	3.0690	1.148
+1.0%	−1.24	2.7711	1.519	−1.49	3.0843	1.157

[a] The pressures are estimated using the Birch-Murnaghan equation of state for bulk. The same dilation was applied in x, y, and z directions simultaneously. For instance, the +1.0% dilation increases the volume by +3.03%.

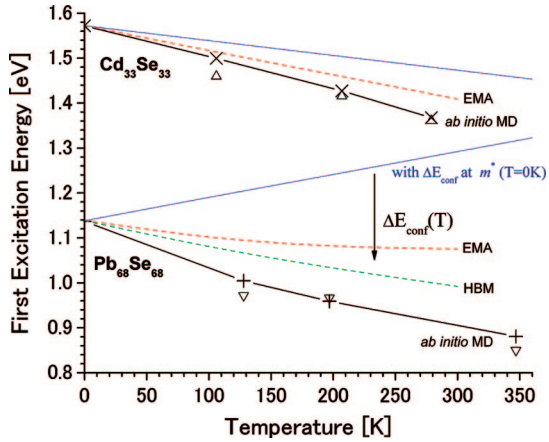

Figure 4. First excitation energies of the CdSe and PbSe QDs as functions of temperature. The dashed lines represent the estimates obtained with eq 6. The blue dotted lines represent the bulk contributions to the same estimates. The crosses represent the simulation data averaged over the entire MD trajectories, and the triangles represent the data averaged over only five randomly selected points along the trajectory.

was obtained in both cases, with the slopes $dE_g/dT = -0.73$ (−0.74) meV/K for the CdSe (PbSe) QDs. Experimental measurements of the band gap of CdSe QDs reported linear temperature dependence as well.[25,33] The literature values are summarized in Table 3 together with the results of the present calculations. The table also shows the experimental dot diameter and temperature range. The experimental data indicate that smaller QDs give larger absolute values of negative dE_g/dT. Taking this into consideration, our results are in accordance with the experiments. Several experiments reported a plateau[25,33] or a drop[23] in the low-temperature region of $T < 100$ K. Such behavior was not found in our calculations.

Figure 5 summarizes the effect of temperature and pressure on the band gap with respect to the average bond length. The bond lengths reported in Table 3 were averaged over all bonded Cd−Se (Pb−Se) pairs. The data of Figure 5 indicate that the change in the band gap cannot be understood simply in terms of the averaged bond length. For QDs under pressure, the behavior of the gap as a function of the bond length is similar to that in the bulk and has different signs for CdSe and PbSe.

TABLE 3: Band Gaps of the CdSe and PbSe QDs Calculated at Different Temperatures[a]

CdSe QD			PbSe QD		
T [K]	⟨r(Cd−Se)⟩ [Å]	E_g [eV]	T [K]	⟨r(Pb−Se)⟩ [Å]	E_g [eV]
0	2.7437	1.572	0	3.0578	1.137
106	2.7500	1.499	128	3.0709	1.005
207	2.7578	1.427	197	3.0770	0.959
279	2.7620	1.367	347	3.0877	0.881

[a] A strong size-dependence of dE_g/dT had been reported for PbSe QDs in ref 26. Figure 4 of this paper shows that dE_g/dT is negative for PbSe QD with diameters smaller than 2.4 nm. The same figure gives an estimate around –0.60 meV/K for the 2 nm PbSe QD, which is similar to the presently studied QD. Our result of –0.74 meV/K agrees with this estimate.

At the same time, the increase of the bond length associated with thermal fluctuations correlates with a decreased gap in both QDs.

Figures 6 and 7 depict the autocorrelation functions $C(t)$, eq 1, and their spectral densities, respectively. The oscillations in Figure 6 correspond to the peaks at 210 cm^{-1} in Figure 7. The frequency coincides with the longitudinal optical (LO) phonon frequency ($\omega_{LO} = 6.1 \times 10^{12}$ Hz = 205 cm^{-1} = 163 fs) reported in ref 64. The initial values of $C(t)$ differ considerably at the three temperatures. However, $C(t)$ are quite close after the first oscillation for all temperatures (Table 4).

Direct evaluation using eq 2 and the cumulant expansion, eq 3, generate very similar optical response functions for the QDs under investigation, as illustrated in Figure 4 of ref 42. In either scheme, a smooth Gaussian profile of the decay was observed. The pure-dephasing/decoherence time was determined from the Gaussian decay: $t = \lambda^{-1/2}$, $D(\tau) \sim e^{-\lambda\tau^2}$. The values are shown in Table 5 and Figure 8. The decoherence time changes almost linearly with temperature. The relative order of the decoherence times for different state pairs is the same as the one established for PbSe at room temperature,[42] with the exception of PbSe at $T = 100$ K.

Discussion

As seen in Figure 3, there are large differences between the band gaps in the QDs and the corresponding bulk. Experimentally, it is known that the first excitonic transition energy goes

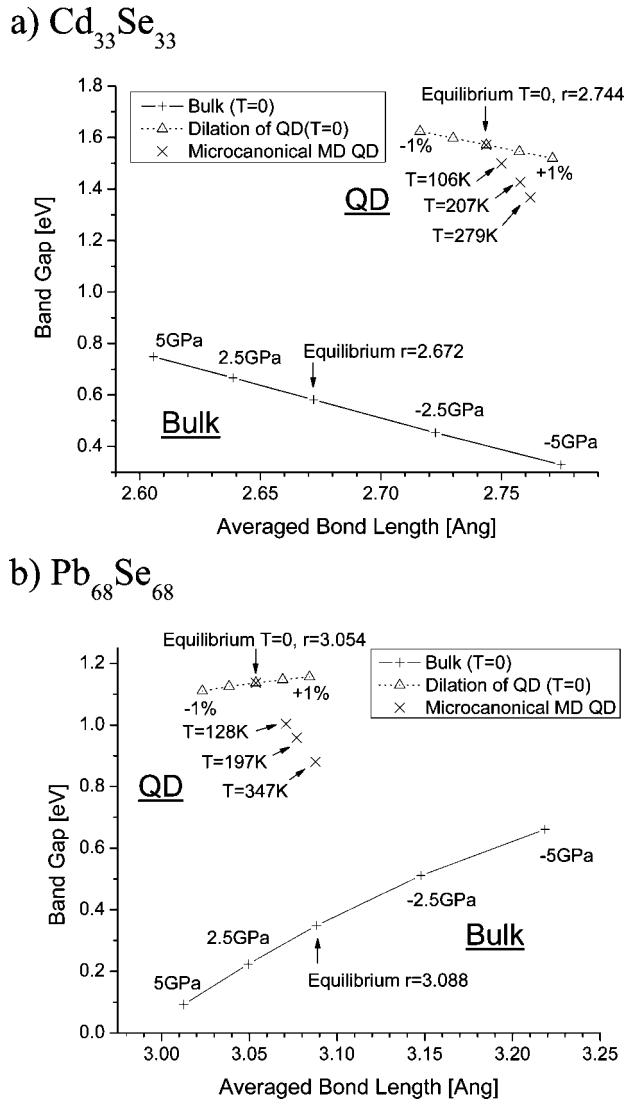

Figure 5. First excitation energies of the CdSe and PbSe QDs as functions of the averaged bond length obtained from the QD dilations and MD simulations at different temperatures.

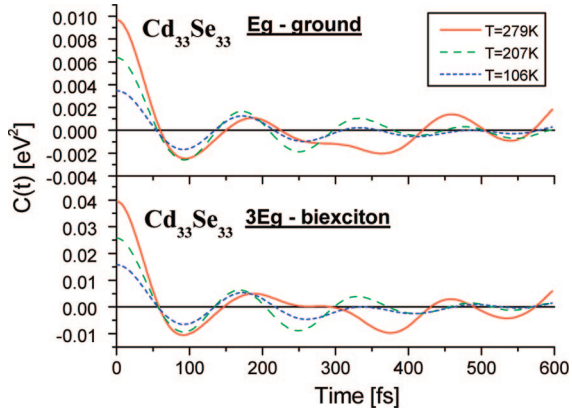

Figure 6. Autocorrelation functions $C(t)$ for the gaps between the lowest energy exciton and the ground state, and a high energy exciton and biexciton in the $Cd_{33}Se_{33}$ QD.

up when the QD size decreases.[65] This change in the band gap is explained by electron confinement in a small region of semiconductor and is known as the confinement energy.

A straightforward estimate of the confinement energy can be made with the effective mass approximation (EMA).[66] In the EMA

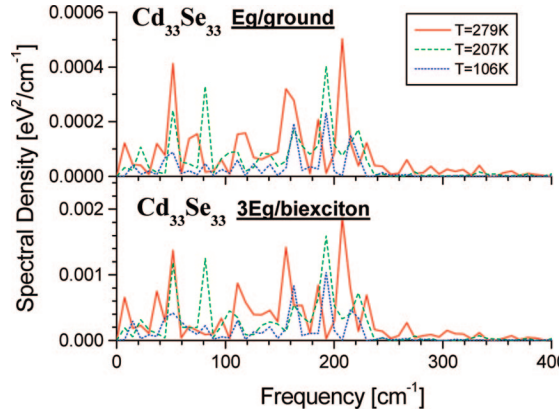

Figure 7. Spectral density of the autocorrelation functions $C(t)$ shown in Figure 6.

TABLE 4: Temperature Dependence of the Band Gap in CdSe QDs of Different Sizes

type of CdSe	T [K]	dE_g/dT [meV/K]	ref
CdSe bulk		−0.28	72
CdSe bulk	100–300	−0.36	33
CdSe/ZnS QD (d = 5.2 nm)	0–300	−0.37	25
CdSe QD (d = 4.0 nm)	235–385	−0.38	24
CdSe QD (d = 2.5 nm)	270–375	−0.51	24
CdSe/ZnS QD (d = 1.9 nm)	0–300	−0.44	25
CdSe QD (d = 1.6 nm)	0–297	−0.73	this study

TABLE 5: Phonon-Induced Pure-Dephasing/Decoherence Time for Pairs of Electronic States

		pure dephasing time, fs		
cluster	state pair	T = 106 K	T = 207 K	T = 279 K
$Cd_{33}Se_{33}$	E_g/ground	16.2	11.2	9.6
	$2E_g/E_g$	17.8	12.1	11.0
	$3E_g/E_g$	13.3	10.7	8.9
	$2E_g$/biexciton	8.9	6.0	5.4
	$3E_g$/biexciton	7.5	5.6	4.8
		pure dephasing time, fs		
cluster	state pair	T = 128 K	T = 197 K	T = 347 K
$Pb_{68}Se_{68}$	E_g/ground	22.6	16.3	9.3
	$2E_g/E_g$	19.0	17.0	10.6
	$3E_g/E_g$	22.4	15.2	8.6
	$2E_g$/biexciton	10.7	8.6	5.3
	$3E_g$/biexciton	11.6	8.1	4.7

model, the QD is treated as a spherical well containing a trapped electron and a hole, which are described by independent effective masses and which interact via a screened Coulomb attraction. In a small QD, the two particles behave independently rather than as exciton, because the kinetic energy of confinement scales as the inverse square of the dot radius r^{-2}, whereas the electron–hole Coulomb interaction scales only inversely with the radius. According to ref 67, the transition between the exciton and independent particle pictures takes place around $4a_0 < R < a_0$ where a_0 is the Bohr radius of the exciton. The a_0 values are 6 and 46 nm for bulk CdSe and PbSe, respectively.[11] The size of dots in the present study, d = 1.6–2.0 nm, is much smaller than these Bohr radii. In such strong confinement regime, the confinement energy can be estimated in the following way:[66]

$$\Delta E_{\mathrm{conf}}^{\mathrm{EMA}} \simeq \frac{\hbar\pi^2}{2r^2}\left[\frac{1}{m_e}+\frac{1}{m_h}\right] - \frac{1.786e^2}{\varepsilon r} + \text{polarization} \quad (4)$$

where r, m_e, m_h, e, and ϵ represent the radius of the dot, the effective mass of the electron, the effective mass of the hole,

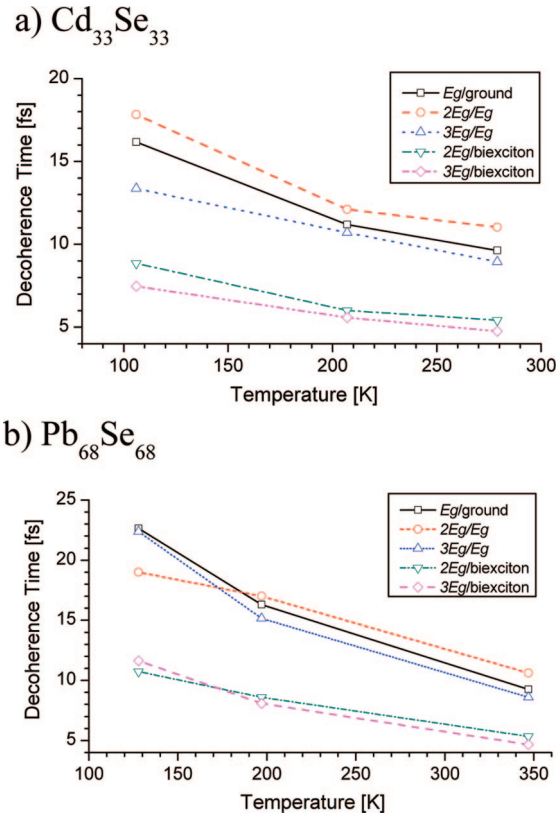

Figure 8. Pure-dephasing/decoherence time between different electronic state pairs as a function of temperature.

the charge of the electron, and the dielectric constant, respectively. The polarization term is much smaller than the first and second terms. Other effects, such as the Coulomb interaction and the triplet-singlet splitting, are much smaller and can be treated as perturbations.[68] The values of the dielectric constants used in this study are 9.2 for CdSe[69] and 23 for PbSe.[68]

An alternative model has been advocated for PbSe QDs in ref 66. Called hyperbolic band model (HBM), it was originally introduced for PbS QD.[66] HBM takes into consideration several properties of the electronic structure of PbS and PbSe, such as the narrow band gap, the emergence of the gap at the L point, and the ionic character of the excitonic state. The expression for the confinement energy is written in HBM as

$$\Delta E_{\mathrm{conf}}^{\mathrm{HBM}} \simeq \sqrt{(E_{\mathrm{g}}^{\mathrm{bulk}})^2 + \frac{2\hbar^2\pi^2}{\mu r^2}E_{\mathrm{g}}^{\mathrm{bulk}}} - E_{\mathrm{g}}^{\mathrm{bulk}} \qquad (5)$$

where $\mu^{-1} = m_{\mathrm{e}}^{-1} + m_{\mathrm{h}}^{-1}$. The last term was used in this paper in order to be consistent with eq 4, which gives zero for $r \rightarrow \infty$.

The QD band gap is expressed as

$$E_{\mathrm{g}}^{\mathrm{QD}}(T,P) \simeq E_{\mathrm{g}}^{\mathrm{bulk}}(T,P) + \Delta E_{\mathrm{conf}}(\mu, r) \qquad (6)$$

where ΔE_{conf} is either $\Delta E_{\mathrm{conf}}^{\mathrm{EMA}}$ or $\Delta E_{\mathrm{conf}}^{\mathrm{HBM}}$ for PbSe and $\Delta E_{\mathrm{conf}}^{\mathrm{EMA}}$ for CdSe.

Direct application of eqs 5 and 6 with the actual value of r overestimates the confinement energy by an order of magnitude for both CdSe and PbSe QDs, within either EMA or HBM. More reliable estimates require more advanced theoretical treatments of the QD electronic structure, such as the four-band model,[68] tight-binding calculations,[70] or the atomistic pseudopotential approach.[71]

In order to compare our *ab initio* results with EMA and HBM, we scaled the radius r^* such that eq 3 matched the *ab initio* confinement energy at $P = 0$ GPa and $T = 0$ K

$$r_{\mathrm{EMA}}^* = 1.44r \quad \text{for CdSe} \qquad (7a)$$

$$r_{\mathrm{EMA}}^* = 4.05r \quad \text{and} \quad r_{\mathrm{HBM}}^* = 2.82r \quad \text{for PbSe} \qquad (7b)$$

A constant shift rather than scaling of the radius was also attempted. There was no qualitative difference in the results between these two definitions, and the agreement to the *ab initio* MD was better with the scaling. The EMA and HBA data presented here were obtained using the scaled radii.

In order to investigate the effect of pressure and temperature on the QD properties, we described the temperature and pressure dependence of the band gap in the bulk as follows:

$$E_{\mathrm{g}}^{\mathrm{bulk}}(T,P) = 0.581 - 3.3\times10^{-4}T + 4.2\times10^{-2}P \quad \text{for CdSe}^{33,72} \qquad (8a)$$

$$E_{\mathrm{g}}^{\mathrm{bulk}}(T,P) = 0.348 + 5.1\times10^{-4}T - 5.7\times10^{-2}P \quad \text{for PbSe}^{73} \qquad (8b)$$

The parameters for the temperature dependences were taken from the literature. The parameters for the pressure dependence were deduced from our calculations. According to ref 73, the lattice dilation of PbSe bulk contributes about half, $+2.7 \times 10^{-4}\ T$, to the overall temperature dependence.

The electron and hole effective masses reported at $T = 300$ K are $0.13m_0$ and $0.45m_0$[74] (0.084 m_0 and 0.070 m_0[68]) for CdSe (PbSe), respectively. m_0 is the free electron mass. Taking the temperature dependence from the theoretical estimate for CdSe[33] and the experimental measurements for PbSe,[75] one can write the following expressions for the average effective mass:

$$\mu(T) = 0.095(1 + 2\times10^{-4}T) \quad \text{for CdSe} \qquad (9a)$$

$$\mu(T) = 0.028(1 + 1.2\times10^{-3}T) \quad \text{for PbSe} \qquad (9b)$$

The coefficients in these two equations indicate that the temperature dependence of the effective mass is stronger in PbSe. All papers cited above as well as our current results for bulk show almost linear behavior for both $E_{\mathrm{g}}^{\mathrm{bulk}}(T, P)$ and $\mu(T)$ in the temperature range $T = 0$–300 K, justifying the validity of the above equations.

In this model, the pressure and temperature dependence of the electronic energy gap in the QDs is described through $E_{\mathrm{g}}^{\mathrm{bulk}}(T, P)$, $\mu(T)$, and r. In principle, $E_{\mathrm{g}}^{\mathrm{bulk}}$ appearing in $\Delta E_{\mathrm{conf}}^{\mathrm{HBM}}$, eq 5, should also depend on pressure and temperature. Instead, $E_{\mathrm{g}}^{\mathrm{bulk}}$ was fixed at 0.348 eV obtained for $P = 0$ GPa and $T = 0$ K. Including the temperature dependence of $E_{\mathrm{g}}^{\mathrm{bulk}}$ in eq 5 significantly changes $\Delta E_{\mathrm{conf}}^{\mathrm{HBM}}$, and the results deviate from the *ab initio* MD results. This may be caused by the error in the absolute value of the gap or by the use of the scaled radius.

The pressure and temperature dependence of the QD energy gaps estimated by the above models is illustrated in Figures 3 and 4 together with the *ab initio* data. The slopes dE_{g}/dP for the CdSe QD and bulk are quite similar. In contrast, the slope is smaller for the PbSe QD than for bulk PbSe. The smaller slope for the PbSe QD indicates that the confinement energy shows opposite pressure dependence than the bulk energy gap. In the models introduced above, the change in ΔE_{conf} emerges from the change in the QD radius. Including pressure dependence of the effective mass may improve the agreement between the model and *ab initio* data.

The blue dotted lines in Figure 4 represent $E_{\mathrm{g}}(T)$ omitting the confinement energy. These lines reveal that the dominant

contributions to dE_g/dT differ between the CdSe and PbSe QDs, nevertheless the net results are quite similar. The temperature dependence of the band gap in the CdSe QD arises primarily from the bulk term. The confinement energy has a significant effect for PbSe QDs. The change of the confinement energy comes from the temperature dependence of the effective mass in eq (9). The change due to the QD radius is small. According to the r^{-2} scaling and the dilation estimates discussed above, the change in the band gap due to QD thermal expansion between $T = 0$ and 300 K should be around ~0.44% (0.004 eV) for CdSe and ~1.2% (0.009 eV) for PbSe.

The effective masses of electron and hole are determined by several factors, including lattice structure, electron correlation and electron–phonon coupling. Yokoi et al. suggested that the temperature dependence of the effective mass in bulk PbSe is determined by the rather peculiar electron–phonon interaction.[75] The present calculation treats the nuclear motion and electron–phonon coupling directly and not as a perturbation. The heavy masses of the Pb and Se atoms and the low vibrational frequencies of PbSe justify the classical treatment. Therefore, the present results can be regarded as a proof for the importance of the temperature dependence of the effective mass, caused by the electron–phonon coupling, as suggested by Liptay et al.[33]

Finally, a few comments are in order regarding the pure-dephasing/decoherence time. Approximately, the decoherence time is shorter than the oscillation period found in $C(t)$ by 1 order of magnitude. This means that decoherence between the electronic states is dominated by the initial value of $C(0)$, which is just the square of the vibrationally induced fluctuation of the electronic energy gap. The contribution of the LO phonons to the electron–phonon coupling is smaller than that of the acoustic phonons.[11] The LO phonon is known to be the source of nonlinear temperature dependence of the excitonic peak broadening.[76]

Conclusions

We investigated the pressure and temperature dependence of the band gap in the $Pb_{68}Se_{68}$ ($d = 2.0$ nm) and $Cd_{33}Se_{33}$ ($d = 1.6$ nm) QDs using ab initio DFT. The dE_g/dP value was 39.8 meV/GPa for CdSe QD and –14.3 meV/GPa for PbSe QD. These values were qualitatively similar to the corresponding bulk values of +42.0 and –56.9 meV/GP, respectively. The absolute magnitude of dE_g/dP was smaller for the PbSe QD than bulk. In contrast, the temperature dependence of the band gap differed significantly for the QDs and bulk, especially for PbSe, where dE_g/dT had opposite signs. To rationalize this finding, a simple model was proposed using two alternative descriptions of the confinement energy. The change of the sign was explained by the temperature dependence of the effective mass in PbSe. Thus, the simulations provided an *ab initio* proof of the analytic models.

The pure-dephasing/decoherence times between several experimentally relevant electronic state pairs were computed using optical response theory and ab initio MD. Linear temperature dependence was found for both QDs. The relative order of the decoherence times for the selected state pairs was similar to the order found in our previous study of the PbSe QD at $T =$ 300 K.

The main advantage of our study is the first-principle description of the electronic states and the electron–phonon coupling. The simulation explicitly includes QD chemical and physical properties, which are not included in the analytic models, but receive close experimental attention. Particularly important are the effects of the QD surface and imperfect symmetry arising from the underlying atomistic structure and thermally induced disorder.

Acknowledgment. H.K. expresses his gratitude for JSPS Research Fellowships for Young Scientists. K.Y. is supported by a Grant-in-aid for The 21st Century COE Program for "Frontiers in Fundamental Chemistry", and for Scientific Research (KAKENHI) in Priority Area "Molecular Theory for Real Systems", from the Ministry of Education, Culture, Sports, Science and Technology of Japan. O.V.P. acknowledges financial support of DOE, Grant No. DE-FG02-05ER15755, and ACS PRF, Grant No. 46722-AC6. We thank Bradley F. Habenicht for comments on the manuscript.

References and Notes

(1) Harbold, J. M.; Du, H.; Krauss, T. D.; Cho, K.-S.; Murray, C. B.; Wise, F. W. *Phys. Rev. B* **2005**, *72*, 195312.
(2) Schleser, R.; Ihn, T.; Ruh, E.; Ensslin, K.; Tews, M.; Pfannkuche, D.; Driscoll, D. C.; Gossard, A. C. *Phys. Rev. Lett.* **2005**, *94*, 206805.
(3) Koppens, F. H. L.; Folk, J. A.; Elzerman, J. M.; Hanson, R.; Willems van Beveren, L. H.; Vink, I. T.; Tranitz, H. P.; Wegscheider, W.; Kouwenhoven, L. P.; Vandersypen, L. M. K. *Science* **2005**, *309*, 1346.
(4) Klimov, V. I.; Mikhailovsky, A. A.; Xu, S.; Malko, A.; Hollingsworth, J. A.; Leatherdale, C. A.; Eisler, H.-J.; Bawendi, M. G. *Science* **2000**, *290*, 314.
(5) Coe, S.; Woo, W. K.; Bawendi, M.; Bulović, V. *Nature* **2002**, *420*, 800.
(6) Talapin, D. V.; Murray, C. B. *Science* **2005**, *310*, 86.
(7) Lu, W.; Fang, J.; Stokes, K. L.; Lin, J. *J. Am. Chem. Soc.* **2004**, *126*, 11798.
(8) Labeau, O.; Tamarat, P.; Lounis, B. *Phys. Rev. Lett.* **2003**, *90*, 257404.
(9) Colvin, V. L.; Cunninghan, K. L.; Alivisatos, A. P. *J. Chem. Phys.* **1994**, *101*, 7122.
(10) Cordero, S. R.; Carson, P. J.; Estabrook, R. A.; Strouse, G. F.; Buratto, S. K. *J. Phys. Chem. B* **2000**, *104*, 12137.
(11) Wise, F. W. *Acc. Chem. Res.* **2000**, *33*, 773.
(12) Califano, M.; Franceschetti, A.; Zunger, A. *Nano Lett.* **2005**, *5*, 2360.
(13) Ellingson, R. J.; Beard, M. C.; Johnson, J. C.; Yu, P.; Mićić, O. I.; Nozik, A. J.; Shabaev, A.; Efros, A. L. *Nano Lett.* **2005**, *5*, 865.
(14) Murphy, J. E.; Beard, M. C.; Norman, A. G.; Ahrenkiel, S. P.; Johnson, J. C.; Yu, P.; Mićić, O. I.; Ellingson, R. J.; Nozik, A. J. *J. Am. Chem. Soc.* **2006**, *128*, 3241.
(15) Nozik, A. J. *Annu. Rev. Phys. Chem.* **2001**, *52*, 193.
(16) Schaller, R. D.; Klimov, V. I. *Phys. Rev. Lett.* **2004**, *92*, 186601.
(17) Schaller, R. D.; Sykora, M.; Pietryga, J. M.; Klimov, V. I. *Nano Lett.* **2006**, *6*, 424.
(18) Li, J.; Li, G.; Xia, J.; Zhang, J.; Lin, Y.; Xiao, X. *J. Phys.: Condens. Matter* **2001**, *13*, 2033.
(19) Meulenberg, R. W.; Strouse, G. F. *Phys. Rev. B* **2002**, *66*, 035317.
(20) Fan, H. M.; Ni, Z. H.; Feng, Y. P.; Fan, X. F.; Kuo, J. L.; Shen, Z. X.; Zou, B. S. *Appl. Phys. Lett.* **2007**, *90*, 021921.
(21) Zhuravlev, K. K.; Pietryga, J. M.; Sander, R. K.; Schaller, R. D. *Appl. Phys. Lett.* **2007**, *90*, 043110.
(22) Nomura, S.; Kobayashi, T. *Phys. Rev. B* **1992**, *45*, 1305.
(23) Salvador, M. R.; Graham, M. W.; Scholes, G. D. *J. Chem. Phys.* **2006**, *125*, 184709.
(24) Dai, Q.; Song, Y.; Li, D.; Chen, H.; Kan, S.; Zou, B.; Wang, Y.; Deng, Y.; Hou, Y.; Yu, S.; Chen, L.; Liu, B.; Zou, G. *Chem. Phys. Lett.* **2007**, *439*, 65.
(25) Joshi, A.; Narsingi, K. Y.; Manasreh, M. O.; Davis, E. A.; Weaver, B. D. *Appl. Phys. Lett.* **2006**, *89*, 131907.
(26) Olkhovets, A.; Hsu, R.-C.; Lipovskii, A.; Wise, F. W. *Phys. Rev. Lett.* **1998**, *81*, 3539.
(27) Fernée, M. J.; Jensen, P.; Rubinsztein-Dunlop, H. *J. Phys. Chem. C* **2007**, *111*, 4984.
(28) Vossmeyer, T.; Katsikas, L.; Giersig, M.; Popovic, I. G.; Diesner, K.; Chemseddine, A.; Eychmüller, A.; Weller, H. *J. Phys. Chem.* **1994**, *98*, 7665.
(29) Fan, H. Y. *Phys. Rev.* **1951**, *82*, 900.
(30) Keffer, C.; Hayes, T. M.; Bienenstock, A. *Phys. Rev. B* **1970**, *2*, 1966.
(31) Schlüter, M.; Martinez, G.; Cohen, M. L. *Phys. Rev. B* **1975**, *12*, 650.
(32) Allen, P. B.; Cardona, M. *Phys. Rev. B* **1983**, *27*, 4760.
(33) Liptay, T. J.; Ram, R. J. *Appl. Phys. Lett.* **2006**, *89*, 223132.

(34) Petta, J. R.; Johnson, A. C.; Taylor, J. M.; Laird, E. A.; Yacoby, A.; Lukin, M. D.; Marcus, C. M.; Hanson, M. P.; Gossard, A. C. *Science* **2005**, *309*, 2180.

(35) Johnson, A. C.; Petta, J. R.; Taylor, J. M.; Yacoby, A.; Lukin, M. D.; Marcus, C. M.; Hanson, M. P.; Gossard, A. C. *Nature* **2005**, *435*, 925.

(36) Golovach, V. N.; Khaetskii, A.; Loss, D. *Phys. Rev. Lett.* **2004**, *93*, 16601.

(37) Yao, W.; Liu, R.-B.; Sham, L. J. *Phys. Rev. B* **2006**, *74*, 195301.

(38) Mukamel, S. Principles of Nonlinear Optical Spectrosocpy; Oxford University Press: New York, 1995.

(39) Rudin, S.; Reinecke, T. L.; Bayer, M. *Phys. Rev. B* **2006**, *74*, 161305.

(40) Muljarov, E. A.; Takagahara, T.; Zimmermann, R. *Phys. Rev. Lett.* **2005**, *95*, 177405.

(41) Mittleman, D. M.; Schoenlein, R. W.; Shiang, J. J.; Colvin, V. L.; Alivisatos, A. P.; Shank, C. V. *Phys. Rev. B* **1994**, *49*, 14435.

(42) Kamisaka, H.; Kilina, S. V.; Yamashita, K.; Prezhdo, O. V. *Nano Lett.* **2006**, *6*, 2295.

(43) Iwanaga, H.; Kunishige, A.; Takeuchi, S. *J. Mater. Sci.* **2000**, *35*, 2451.

(44) Madelung, O.; Schulz, M.; Weiss, H. Numerical Data and Functional Relationships in Science and Technology Landolt-Bornstein; Springer: Berlin, 1983; New Series, Vol. 17.

(45) Hohenberg, P.; Kohn, W. *Phys. Rev.* **1964**, *136*, B864.

(46) Kohn, W.; Sham, L. J. *Phys. Rev.* **1965**, *140*, A1133.

(47) Perdew, J. P.; Chevary, J. A.; Vosko, S. H.; Jackson, K. A.; Pederson, M. R.; Singh, D. J.; Fiolhais, C. *Phys. Rev. B* **1992**, *46*, 6671.

(48) Vanderbilt, D. *Phys. Rev. B* **1990**, *41*, 7892.

(49) Kresse, G.; Hafner, J. *J. Phys.: Condens. Matter* **1994**, *6*, 8245.

(50) Kresse, G.; Hafner, J. *Phys. Rev. B* **1993**, *47*, 558.

(51) Edwards, A. L.; Drickamer, H. G. *Phys. Rev.* **1961**, *122*, 1149.

(52) Monkhorst, H. J.; Pack, J. D. *Phys. Rev. B* **1976**, *13*, 5188.

(53) Schröer, P.; Krüger, P.; Pollmann, J. *Phys. Rev. B* **1993**, *48*, 18264.

(54) Wei, S.-H.; Zunger, A. *Phys. Rev. B* **1997**, *55*, 13605.

(55) Albanesi, E. A.; Okoye, C. M. I.; Rodriguez, C. O. Blanca, E. L. P. y.; Petukhov, A. G. *Phys. Rev. B* **2000**, *61*, 16589.

(56) Nabi, Z.; Abbar, B.; Méçabih, S.; Khalfi, A.; Amrane, N. *Comput. Mater. Sci.* **2000**, *18*, 127.

(57) Kilina, S. V.; Craig, C. F.; Kilin, D. S.; Prezhdo, O. V. *J. Phys. Chem. C* **2007**, *111*, 4871.

(58) Neumann, H. *Krist. Tech.* **1980**, *15*, 849.

(59) Shan, W.; Walukiewicz, W.; Ager, J. W., III; Yu, K. M.; Wu, J. *Appl. Phys. Lett.* **2004**, *84*, 67.

(60) Lach-hab, M.; Papaconstantopoulos, D. A.; Mehl, M. J. *J. Phys. Chem. Sol.* **2002**, *63*, 833.

(61) Dornhaus, R.; Nimtz, G.; Schlicht, B. Narrow-gap semiconductors; Springer: New York, 1985.

(62) Suzuki, N.; Sawai, K.; Adachi, S. *J. Appl. Phys.* **1995**, *77*, 1249.

(63) Zakharov, O.; Rubio, A.; Cohen, M. L. *Phys. Rev. B* **1995**, *51*, 4926.

(64) Alivisatos, A. P.; Harris, T. D.; Carroll, P. J.; Steigerwald, M. L.; Brus, L. E. *J. Chem. Phys.* **1989**, *90*, 3463.

(65) Ekimov, A. I.; Efros, A. L.; Onushchenko, A. A. *Solid State Commun.* **1985**, *56*, 921.

(66) Wang, Y.; Suna, A.; Mahler, W.; Kasowski, R. *J. Chem. Phys.* **1987**, *87*, 7315.

(67) Kayanuma, Y. *Phys. Rev. B* **1988**, *38*, 9797.

(68) Kang, I.; Wise, F. W. *J. Opt. Soc. Am. B* **1997**, *14*, 1632.

(69) Laheld, U. E. H.; Einevoll, G. T. *Phys. Rev. B* **1997**, *55*, 5184.

(70) Allan, G.; Delerue, C. *Phys. Rev. B* **2004**, *70*, 245321.

(71) Franceschetti, A.; Fu, H.; Wang, L. W.; Zunger, A. *Phys. Rev. B* **1999**, *60*, 1819.

(72) Kim, B. S.; Islam, M. A.; Brus, L. E.; Herman, I. P. *J. Appl. Phys.* **2001**, *89*, 8127.

(73) Baleva, M.; Georgiev, T.; Lashkarev, G. *J. Phys.: Condens. Matter* **1990**, *1*, 2935.

(74) Menéndez-Proupin, E.; Trallero-Giner, C. *Phys. Rev. B* **2004**, *69*, 125336.

(75) Yokoi, H.; Takeyama, S.; Portugall, O.; Miura, N.; Bauer, G. *Physica B* **1993**, *184*, 173.

(76) Valerini, D.; Cretí, A.; Lomascolo, M. *Phys. Rev. B* **2005**, *71*, 235409.

JP710435Q